

This is the accepted manuscript made available via CHORUS. The article has been published as:

Microwave pinning modes near Landau filling $\nu=1$ in two-dimensional electron systems with alloy disorder

B.-H. Moon, L. W. Engel, D. C. Tsui, L. N. Pfeiffer, and K. W. West

Phys. Rev. B **92**, 035121 — Published 9 July 2015

DOI: [10.1103/PhysRevB.92.035121](https://doi.org/10.1103/PhysRevB.92.035121)

Microwave pinning modes near Landau filling $\nu = 1$ in two-dimensional electron systems with alloy disorder

B.-H. Moon,¹ L. W. Engel,¹ D. C. Tsui,² L. N. Pfeiffer,² and K. W. West²

¹*National High Magnetic Field Laboratory,
1800 E. Paul Dirac Drive, Tallahassee, FL 32310*

²*Department of Electrical Engineering,
Princeton University, Princeton, NJ 08544*

(Dated: June 12, 2015)

Abstract

We report measurements of microwave spectra of two-dimensional electron systems hosted in dilute Al alloy, $\text{Al}_x\text{Ga}_{1-x}\text{As}$, for a range of Landau level fillings, ν , around 1. For $\nu > 0.8$ or $\nu < 1.2$, the samples exhibit a microwave resonance whose frequency decreases as ν moves away from 1. A resonance with this behavior is the signature of solids of quasiparticles or -holes in the partially occupied Landau level, and was previously seen only in ultralow disorder samples. For $\nu < 0.8$ down to as low as $\nu = 0.54$, a resonance in the spectra is still present in the Al alloy-disordered samples, though it is partially or completely suppressed at $\nu = 3/5$ and $1/2$, and is strongly damped over much of this ν range. The resonance also shows a striking enhancement in peak frequency for ν just below $3/4$. We discuss possible explanations of the resonance behavior for $\nu < 0.8$ in terms of the composite fermion picture.

In two-dimensional electron systems (2DES) in high magnetic field, B , Wigner solids^{1–20} pinned by residual disorder occur for sufficiently small Landau level filling factor, ν . At the low- ν termination of the fractional quantum Hall effect (FQHE) series, such a solid can appear in dc transport as an insulating phase. By means of microwave spectroscopy like that employed to obtain the data in this paper, Wigner solids of dilute quasiparticles or quasiholes in the presence of one or more filled Landau levels have also been found^{21–25} in extremely high mobility, low disorder 2DES. This type of solid has been named an integer quantum Hall effect Wigner solid (IQHEWS) since the vanishing diagonal conductivity in the wings of the integer quantum Hall effect (IQHE) diagonal conductivity minimum is due to the pinning of the solid. An analogous solid composed of quasiparticles and -holes of the $1/3$ fractional quantum Hall liquid has also been reported²⁶.

Microwave spectroscopy is known to directly measure pinned solids in high magnetic field, since these solids exhibit resonances in their microwave spectra^{10,13,16,17,21–23,26,27}. The resonances are understood as pinning modes^{13–18,28}, in which pieces of the solid oscillate within the disorder potential. The relation between the disorder and the resonance frequency and lineshape is only partially understood. It is clear though, that both the spatial frequency spectrum of the disorder and its strength figure into the frequency, f_{pk} , of the resonance, as do the density of the Wigner solid and its elastic properties. In weak pinning^{28–31}, an increase in the disorder potential or a decrease in the crystal stiffness decreases the correlation length of crystalline order, and also increases f_{pk} . If the disorder becomes so strong that the positions of the carriers are no longer sensitive to the crystal stiffness, then strong pinning results²⁸ as long as the disorder consists of pinning centers many lattice constants apart. The pinned-solid description of the 2DES would not hold if the disorder correlation length is shorter and the disorder potential completely overwhelms the electron-electron interaction (so that a small displacement of a single carrier would not affect the positions of its neighbors). The spatial frequency and strength of disorder required to destroy the solid are not known. This paper sheds light on the problem by presenting a case for which a component of the disorder is known, and for which the spectra are consistent with a pinned solid.

In weak pinning the lower f_{pk} results for a stiffer solid because³¹ the carriers of the stiffer solid stay closer to positions that minimize the interelectron repulsion, rather than positions at minima in the disorder potential. Increasing the charge density of the solid makes it stiffer and reduces f_{pk} , as was shown experimentally for the low ν solid phase^{17,18} using a

backgate to change the density. The filling factor of the carriers that form the IQHEWS is $|\nu - J|$, where J is the filling at the center of the plateau. As $|\nu - J|$ increases, the density of the solid, $n^* = |\nu - J|n/\nu$, increases, and f_{pk} decreases, as shown by experiments^{21–23}. For ν above 1.15 or below 0.85 in low disorder samples²¹, the resonance fades away as the carriers become dense enough for the solid to melt.

All earlier reports^{21–25} of IQHEWS have been on samples of the highest quality. These samples include²² a 50 nm quantum well, with mobility $\mu \approx 15 \times 10^6$ cm²/V-s, and a 30 nm well^{21,22} with $\mu \approx 27 \times 10^6$ cm²/V-s. Here we report IQHEWS, identified from microwave spectroscopy, in samples with far lower mobility, 1.4 and 2.3×10^6 cm²/V-s. The samples used in this work contain the 2DES in dilute Al alloy, $\text{Al}_x\text{Ga}_{1-x}\text{As}$, so the isoelectronic Al impurities provide an additional component of the overall disorder. This additional component of disorder has been characterized precisely³³ in a study of mobility vs x and temperature. The length scales of this disorder potential are much less than the magnetic length, l_B , under all conditions in this paper. The case of the IQHEWS provides a way to vary the density of the solid simply by varying the magnetic field, and to observe IQHEWS and other Wigner solids in the presence of a filled Landau level.

This paper shows that even with the Al alloy disorder, the resonances can exhibit the behavior expected of an IQHEWS, with f_{pk} increasing as $\nu = 1$ is approached. f_{pk} vs ν also shows inflections possibly due to skyrmion crystallization²². Furthermore, more detailed study of the pinning resonance also shows that relative to samples without Al, the resonance range is greatly extended on the hole side ($\nu < 1$) down to $\nu \sim 0.6$. In this extended range, the behavior of the resonances is more complex than was reported²¹ in Al-free samples, and the interpretation may require phase transitions within the solid. As ν decreases below 0.8, the trend of decreasing f_{pk} reverses, and f_{pk} vs ν develops a strongly disorder-dependent maximum for ν just below $3/4$. The resonance also is suppressed or partly suppressed at $\nu = 2/3$ and $3/5$. Particularly away from $\nu = 1$ and from the maximum in f_{pk} vs ν , the resonance is highly damped with a rapid rise at low frequency, f , in real diagonal conductivity, $\text{Re}(\sigma_{xx})(f)$. We observed such a highly damped resonance in the ranges of ν between $2/3$ and $3/5$ reported³² to exhibit insulating behavior in the partially filled Landau level in dc transport.

We present data from two samples with $\text{Al}_x\text{Ga}_{1-x}\text{As}$ channels. Samples from the same wafers were used in earlier work in dc transport^{32–36}. Characterization³³ of the samples at

$B = 0$ showed that the spatial distribution of the Al is random. Both samples are single heterojunctions with the 2DES approximately 180 nm below the top surface of the sample. One sample has $x = 0.33\%$, density $n \approx 2.1 \times 10^{11} \text{ cm}^{-2}$ and as-cooled mobility μ about $2.3 \times 10^6 \text{ cm}^2/\text{V-s}$; the other sample has $x = 0.85\%$, $n \approx 2.5 \times 10^{11} \text{ cm}^{-2}$ and $\mu \approx 1.4 \times 10^6 \text{ cm}^2/\text{V-s}$. A previous paper³⁷ showed that samples from this series exhibit pinning mode resonances at the low ν termination of the FQHE series, which for these disordered samples occurred for ν below that of the $1/3$ FQHE. The presence of disorder is known¹⁶ to raise the ν at which the FQHE series is terminated in an insulator. At least for samples grown in the same series, for which the component of disorder not due to the Al was the same, additional Al raised f_{pk} , as one would expect for a pinning mode.

Microwave spectra of the complex diagonal conductivity σ_{xx} , were obtained from the propagation characteristics of a transmission line¹⁰ that is capacitively coupled to the 2DES. The transmission line we used is shown schematically in Fig. 1a. The lines are of the coplanar waveguide (CPW) type^{17,18,21–23,26,27,39}, with a center conductor separated from two broad ground planes by slots of width $W = 30 \text{ }\mu\text{m}$, and are patterned directly onto the top of the sample. We present complex diagonal conductivity calculated from the model of ref. 39 for the CPW coupled to the 2DES. The results are within about 25% of those from the high frequency low loss approximation, $\sigma_{xx} \approx -W|\ln(s)|/Z_0d$, where s is a complex transmission coefficient, $Z_0 = 50 \text{ }\Omega$ is the characteristic impedance calculated from the transmission line geometry for $\sigma_{xx} = 0$, and d is the length of the coplanar waveguide ($d = 28 \text{ mm}$). s is normalized to the transmission at $\nu = 1$, at which σ_{xx} vanishes due to the IQHE. For all measurements, the 2DES temperature was approximately 60 mK, as read by nearby resistance thermometers. Slight broadening of the resonance could be discerned on increasing the temperature above that value. We verify that the data were taken in the low microwave power limit, in which further decrease of power does not affect the measured spectrum.

First, we show $\text{Re}(\sigma_{xx})$ vs B , to show the development of the quantum Hall effects. Taken at a low frequency of 100 MHz, the data presented in this way allow easy identification of features associated with the FQHE. In what follows, we will show that the pinning modes are at least partly suppressed at rational fractional fillings $3/5$ and $2/3$, showing a competition between the resonant, solid states and the FQHE's. Figure 1b shows $\text{Re}(\sigma_{xx})$ vs B for the two samples. $\text{Re}(\sigma_{xx})$ for the $x = 0.33\%$ sample shows a broad minimum at the $\nu = 1$ IQHE,

and FQHE minima at $3/5, 2/3, 4/3, 7/5, 8/5$ and $5/3$. The curve is composed of points read off from spectra taken at discrete B , and the low density of points gives the traces an artifactual jagged appearance near $\nu = 3/5$ and $2/3$. The width of the IQHE minimum is about 0.3 in ν , measured from halfway up the rises on either side. The trace from the $x = 0.85\%$ sample shows a much wider IQHE around $\nu = 1$, with ν -width measured the same way of 0.56. The FQHE at $2/3$ or $3/5$ is not apparent, though there are minima near $4/3$ and $5/3$. For both traces, the $\nu = 2$ IQHE minimum is well-developed but appears at $\text{Re}(\sigma_{xx})$ slightly elevated from that at $\nu = 1$; we ascribe this to weak, B -dependent parallel conduction in the wafers.

We provide image plots to clearly show the ν range, greatly extended from the ultralow disorder case²¹, in which resonances exist in the spectra, and to highlight the surprisingly complicated development of those resonances in that extended range. Figure 2a is an image plot of spectra, $\text{Re}(\sigma_{xx})$ vs f , on the ν - f plane, for ν between 0.6 and 1.4 for the $x = 0.33\%$ sample. (The $x = 0.33\%$ trace in Fig. 1b is a 0.1 GHz cut of this image.) There are clear resonances on each side on $\nu = 1$, which decrease in f_{pk} as ν moves farther from 1. As ν goes above 1.2, the resonance fades into a flat spectrum. In contrast, as ν goes below 0.8, $\text{Re}(\sigma_{xx})$ vs f continues to exhibit maxima.

Plots of $\text{Re}(\sigma_{xx})$ vs f at several ν present some of the same data as the image plot, but show the details of the resonance line shape, which can be highly asymmetric. The spectra at rational fractional fillings allow us to assess the affect of FQHE states on the resonance. $\text{Re}(\sigma_{xx})$ spectra for all $\nu \leq 1$ and $x = 0.33\%$ are shown in Fig. 3a. For ν between 0.8 and $2/3$, $\text{Re}(\sigma_{xx})$ shows a strongly asymmetric peak, with rapid rise at low f and a high f tail, whose extent is ν dependent. At $2/3$ the spectrum becomes flat. The asymmetric peak reappears for $\nu < 2/3$, but weakens for the lowest ν trace at $\nu = 0.61$.

The development of the resonance with ν for the $x = 0.85\%$ sample is shown as a color image in Fig. 2b, and as selected $\text{Re}(\sigma_{xx})$ vs f curves in Fig. 4a. We again focus on resonance asymmetry and on the behavior of the resonance at rational fractional fillings. Between $\nu = 1.05$ and 1.2, and also between $\nu = 0.94$ and 0.8 there is a resonance whose f_{pk} increases as $\nu = 1$ is approached. As ν goes below 0.8, the resonance moves to strikingly higher f_{pk} , with a maximum f_{pk} around $\nu = 0.74$. As $2/3$ is approached from higher ν the resonance decreases in frequency and gradually becomes asymmetric. A resonance is present at $2/3$ and $3/5$, , but these rational fractional ν are easily distinguished in Fig. 2b by their

reduced overall $\text{Re}(\sigma_{xx})$.

To characterize the spectra, and to summarize the evolution of the resonance with ν for different samples, it is useful to perform fits to extract resonance parameters. Particularly when the resonances are asymmetric and broad, the fits can show smaller trends that are hard to notice in the raw spectra. We found it convenient to fit to the imaginary part of the measured conductivity, since it gives less error for f_{pk} . The fits are demonstrated in figures 3b and 4b, which show $\text{Im}(\sigma_{xx})$ vs f at several fillings as marked. The $\text{Im}(\sigma_{xx})$ spectra can be fit to the imaginary part of the response of a Drude-Lorentz harmonic oscillator⁴⁰, $\sigma_{xx}(f) = \{\sigma_0 f \Delta f / [f \Delta f + i(f^2 - f_{\text{pk}}^2)]\}$, a form commonly used⁴⁰ for dielectrics, where the parameters σ_0 and Δf are the amplitude and line width. The corresponding real part, with the same fit parameters, fit the $\text{Re}(\sigma_{xx})$ spectra to within frequency-independent additive constants. The fit was chosen empirically, and is not readily connected to theoretically derived forms²⁹ of pinning modes for weak disorder in high B , possibly since these existing theories are specific to the weak-disorder limit.

The results of the fits summarize the development of the resonance as ν is varied, and are presented in Fig. 5, which shows f_{pk} and the linewidth, Δf , vs ν and the quasiparticle filling ($\nu^* = \nu - 1$) for both the samples. Both f_{pk} and Δf come from fits of $\text{Im}(\sigma_{xx})$ vs f , like those shown in Fig. 3 and Fig. 4. Figure 5a also shows f_{pk} vs ν from ref. 22, for an ultralow-disorder quantum-well sample with $x = 0$, $n = 2.7 \times 10^{11} \text{ cm}^{-2}$ and $\mu \approx 27 \times 10^6 \text{ m}^2/\text{V-s}$. The $x = 0.33$ and 0.85% f_{pk} traces are decreasing as ν moves away from 1, until ν is about 0.2 away from 1. f_{pk} vs ν for the $x = 0$ ultralow disorder sample likewise decreases on moving away from 1, though in that data set resonance disappears, approximately for $\nu < 0.85$ and $\nu > 1.15$. For the $x = 0.33\%$ f_{pk} vs ν data in Fig. 5a, there are clear inflections at $\nu = 0.91$ and 1.08 . Weaker inflections are also visible in the $x = 0$ f_{pk} vs ν , for ν a little closer to $\nu = 1$. In Fig. 5b a weak inflection at $\nu \approx 0.88$ is also marked in f_{pk} vs ν for $x = 0.85\%$.

The main point of this paper is that the behavior of the resonance when ν is within 0.2 of 1, with f_{pk} decreasing as ν moves away from 1 is evidence for an IQHEWS much like that found²¹ in ultralow disorder samples. The decrease in f_{pk} is due to the increase in quasiparticle or -hole density, which results in a stiffer solid that avoids features of the disorder which increase pinning. f_{pk} is larger than the it is in the ultralow disorder sample, as expected for larger disorder. However the disorder, possibly because of its homogenous

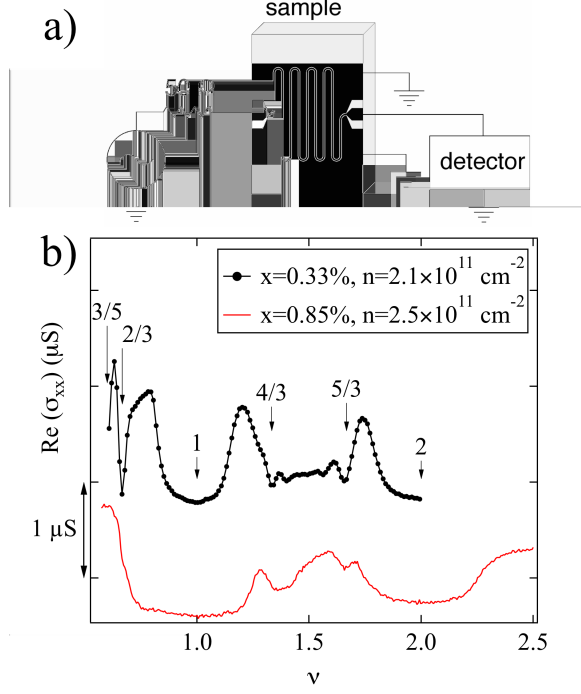


FIG. 1: a) Schematic representation of the microwave circuit used in our measurement, not to scale. Black areas represent metal films on the sample surface. b) Real part of diagonal conductivity $\text{Re}(\sigma_{xx})$, vs Landau filling factor ν for the two samples at 0.1 GHz. The upper, ($x = 0.33\%$) curve was interpolated from spectra, and has a lower density of data points, which are shown as dots.

distribution and short range, still allows IQHEWS formation.

The inflections in the f_{pk} vs ν traces of Fig. 5, most clearly for $x = 0.33\%$, are similar to effects seen in the $x = 0$ ultralow disorder samples studied in ref. 22. The inflections can be regarded as due to a sudden decrease in the pinning as ν approaches 1, superposed on the pinning increase arising from the reduction in quasiparticle density. Based on ref. 22 we could interpret this as consistent with formation of skyrmions^{41–43} containing multiple spins. Crystals^{44,45} of such skyrmions can form near $\nu = 1$ state when 1) ν is sufficiently close to 1 and 2) when Zeeman energy is sufficiently small relative to Coulomb energy, that is, for sufficiently small $\tilde{g} = g\mu_B B_T / (e^2 / 4\pi\epsilon_0 l_B)$, where B_T is total magnetic field. For the $x = 0.33, 0.85\%$ samples, $\tilde{g} = 0.017, 0.019$ respectively, using $|g| = 0.44$. The ultralow-disorder sample that produced the $x = 0$ trace of Fig. 5a had $\tilde{g} = 0.019$ in perpendicular magnetic field; the inflections in f_{pk} vs ν of this sample were shown²² to disappear on applying in-plane magnetic field to increase \tilde{g} . In-plane field experiments on the alloy-

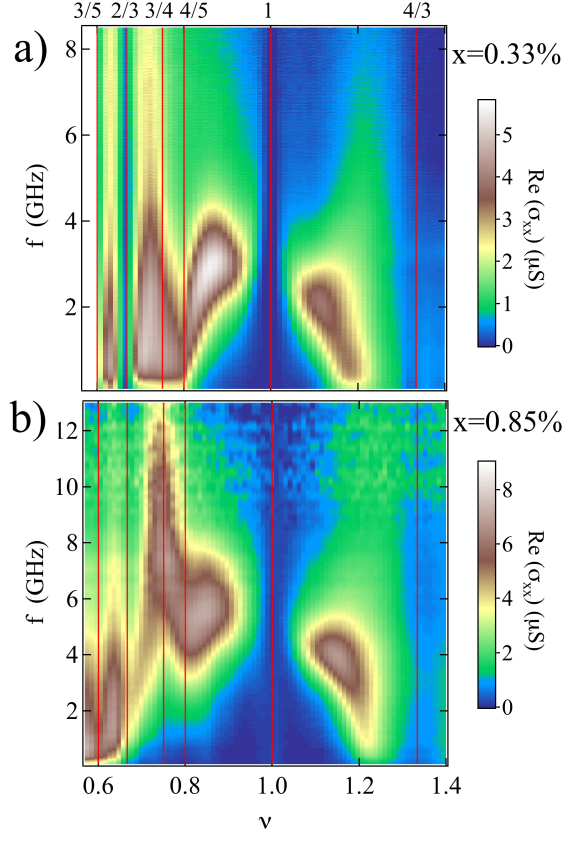


FIG. 2: Color-scale plots showing $\text{Re}(\sigma_{xx})$ in f - ν plane a) $x = 0.33\%$ b) $x = 0.85\%$ Red vertical lines mark Landau filling factors $3/5, 2/3, 3/4, 1$ and $4/3$.

disordered samples would verify the skyrmion based interpretation. The disorder at the $x = 0.33\%$ level appears to make the skyrmion effect *more prominent* than in the $x = 0$ ultralow disorder sample. A skyrmion effect in the Al disordered sample also indicates a remarkable robustness of this interaction-driven phenomenon in the presence of homogenous short-range disorder. While skyrmion crystal formation is a natural interpretation of the inflections, we do not regard that picture to be established definitively for Al alloy-disordered samples until these are studied systematically with in-plane field and varying densities.

We now turn to explanations of the features of the resonance for ν farther than 0.2 from $\nu = 1$. Within this “extended” ν -range, existence of a resonance is a manifestation of the Al disorder, since ultralow-disorder samples do not have a resonance. An explanation⁴⁶ of the extended ν range is that in the competition between solid and FQHE liquids, the solid can be more stable in larger disorder due its pinning energy, which the solid gains as carrier positions adjust to the disorder potential. This is also the explanation for the transition

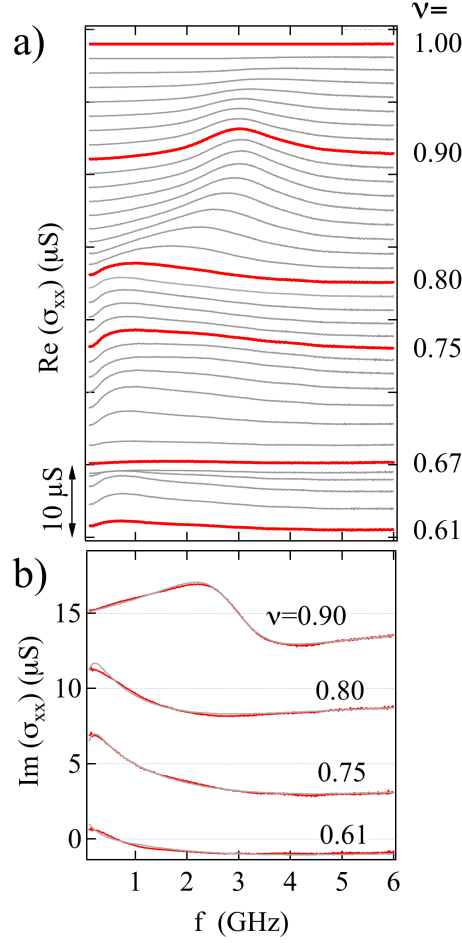


FIG. 3: Spectra for the sample with $x = 0.33\%$ for different Landau level fillings ν . a) $\text{Re}(\sigma_{xx})$ vs frequency, f . Successive spectra were taken at ν -intervals of 0.0107, and are offset vertically proportionally to ν . Landau fillings of certain spectra (red) are marked at right. b) $\text{Im}(\sigma_{xx})$ vs f for several ν . Successive spectra are offset by 5 μS . Fits are light lines, data are darker (red) lines.

to insulator at the low ν termination of the FQHE series occurring around $\nu = 1/3$ in Al alloy-disordered samples^{32,37} (as opposed to near $1/5$ in ultralow disorder samples⁸). The resonance also sets in as ν goes below $1/3$ in low-density samples⁴⁷ or in which the pinning energy is presumably more important relative to the carrier interaction.

Solids can occur reentrantly⁸, for ν above and below the ν -range of an FQHE. Earlier dc transport measurements³² on a sample from the same $x = 0.85\%$ wafer that we consider here, showed a reentrant integer quantum Hall effect (RIQHE) between the $2/3$ and $3/5$ FQHEs. An RIQHE has vanishing diagonal resistance and Hall resistance quantized to

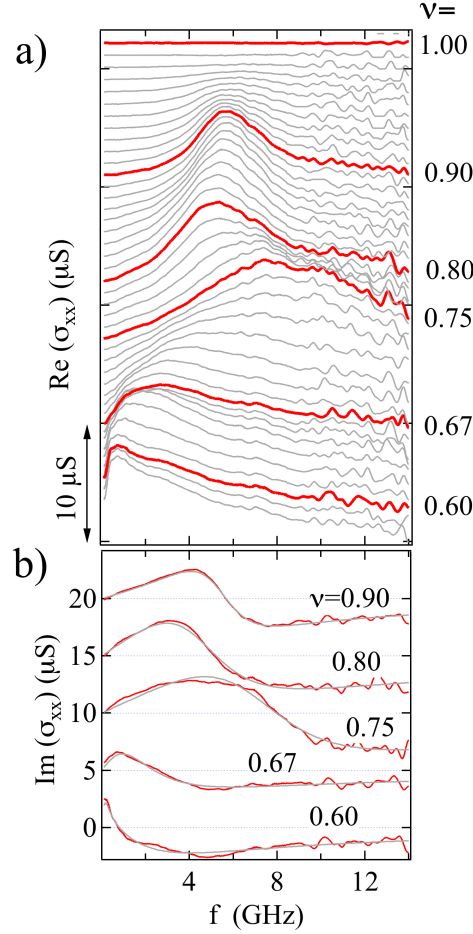


FIG. 4: a) Spectra for the sample with $x = 0.85\%$ for different Landau level fillings ν . a) $\text{Re}(\sigma_{xx})$ vs frequency, f . Successive spectra were taken at ν -intervals of 0.0111, and are offset vertically proportionally to ν . Landau fillings of certain spectra (red on line) are marked at right. b) $\text{Im}(\sigma_{xx})$ vs f for several ν . Successive spectra are offset by $5 \mu\text{S}$. Fits are light lines, data are darker (red on line) lines.

h/e^2 , and indicates the insulating behavior that is expected for a pinned solid of carriers in the partially occupied lowest Landau level. The interpretation of the RIQHE as due to a pinned solid is roughly corroborated by our measurements with the resonance taken as the signature of the pinned solid. We find resonances of the strongly overdamped type in both our samples at the fillings where the RIQHE was located in ref. 32. Possibly because of sample processing, variation within the wafer, or cooldown procedure, we do not find a $2/3$ FQHE suppressing the resonance completely in the present $x = 0.85\%$ sample. In our

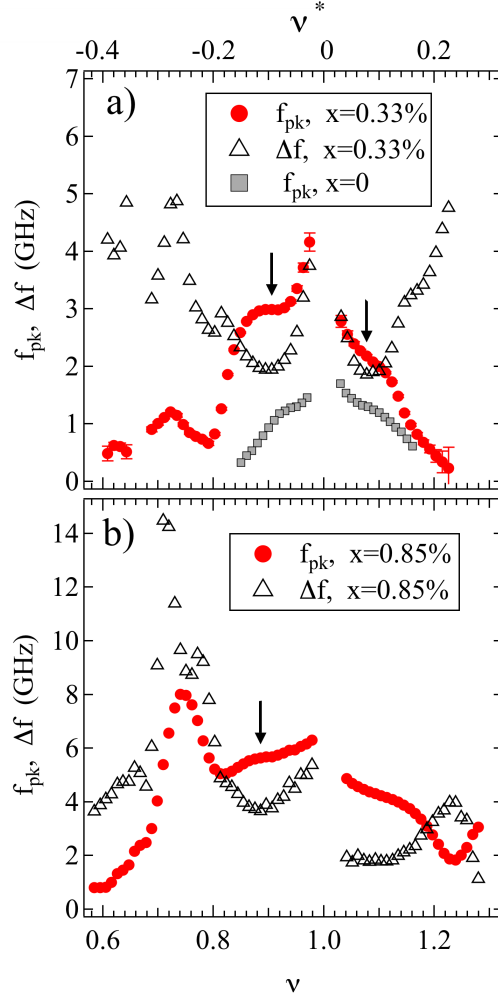


FIG. 5: a) Resonance parameters peak frequency, (f_{pk}) and linewidth, (Δf) vs Landau level filling ν . The quasiparticle filling $\nu^* = \nu - 1$ is shown on the top axis. for a) $x = 0.33\%$, $x = 0$ data are f_{pk} from ref. 22, for a 30 nm quantum well with mobility $27 \times 10^6 \text{ m}^2/\text{V-s}$. b) $x = 0.85\%$. Arrows mark the inflections discussed in the text.

$x = 0.33\%$ sample, there is a $2/3$ FQHE that completely suppresses the resonance.

Other aspects of the resonance in the extended ν range are 1) the dependence of f_{pk} on ν and 2) the comparatively highly damped resonance spectra. While there is no detailed theory to address these phenomena, we will present different possibilities involving the composite fermion (CF) picture⁴⁸.

We first address the nonmonotonic dependence of f_{pk} on ν . In particular, for $\nu < 0.8$, f_{pk} increases with decreasing ν and develops a peak around 0.72 for $x = 0.33\%$, and a much more

pronounced peak around $\nu = 0.74$ for $x = 0.85\%$. There may be some connection between this behavior and recently predicted transitions^{6,7} between different types of Wigner solid. Refs. 6,7 considered composite fermion (CF) Wigner crystals in disorder-free systems, with a CF Wigner crystal, denoted $^{2p}\text{CFWC}$, composed of CFs with $2p$ flux bound to an electron. The theory, presented in ref. 7 for $\nu < 4/17$, predicts a series of transitions between different $^{2p}\text{CFWC}$ with $2p$ increasing as ν decreases, in particular a change from a $^2\text{CFWC}$ to $^4\text{CFWC}$ as ν decreases from $1/5$ to $1/6$. The locations of the observed peaks in f_{pk} vs ν are not covered by the theory (using partial fillings $|\nu^*|$ to compare with ν in the theory). It may be that CF vortex number transitions, if present in these samples, are strongly affected by the disorder, or by the nearly filled lowest Landau level, so that the transitions occur at fillings different than those predicted.

Integral to the CF picture is the formation of Fermi surfaces at even denominator ν ^{48,49}. We speculate that this may relate to the striking maxima in f_{pk} vs ν around $\nu = 0.72$ to 0.74 . These fillings are not far from $\nu = 3/4$ where $2p = 4$ CFs form a Fermi surface, and move in a zero effective magnetic field. It may be that this region is characterized by a CF solid more like a Wigner crystal considered for $B = 0$ ⁵⁰, in which the particle size is determined by competition between kinetic energy and interaction; such a solid would need to be stabilized by the dense homogenous disorder.

We now consider the resonance lineshapes in the extended ν range, which are qualitatively different from those of the better-developed resonances seen closer to integer ν . The overdamped lineshape is unique to the alloy-disordered samples in the extended ν range; the resonances are more symmetric and sharper in the low- ν insulator³⁷ of Al disordered samples, and in both the IQHEWS^{21,22} and the low- ν insulators¹⁸ of samples without deliberately added disorder. The most strongly overdamped resonance spectra reported here are found for ν well below 1, for $\nu < 0.8$ for $x = 0.33\%$ and $\nu < 2/3$ for $x = 0.85\%$, and at low f have $\text{Re}(\sigma_{xx})$ increasing sharply with f . In the ν regions where these spectra occur, the brown color in Fig. 2 comes to within 0.1 GHz of the lower axis. One possible cause of the large damping would be pockets of FQH liquid within the insulating phase. The FQHE liquids are more favored as ν gets farther from 1, so this is consistent with our finding the overdamped resonances in the extended ν range. It is unlikely the pockets are localized in the Al disorder, though it may be that the much weaker, large-length-scale disorder associated with the remote ionized donors is containing liquid pockets, as described in ref. 51. An

inhomogeneous microemulsion phase of the sort proposed in refs. 52,53 is also conceivable. If there are pockets of CF liquid, the additional damping for $\nu \sim 3/4$ is explainable as due to dissipation in the liquid pockets. The dissipation can be larger when there is a Fermi surface. The increase of f_{pk} near that filling could involve the pockets screening the Coulomb interaction between carriers of the solid, reducing its effective stiffness at long range.

In summary we have found that Al-alloy disordered samples exhibit the signature of an IQHEWS for ν within 0.2 of $\nu = 1$. The IQHEWS is remarkably similar to that in ultralow disorder samples, and shows some likely effects of skyrmions. For $\nu < 0.8$, where resonances are not seen for ultralow disorder samples, the resonance has an evolution that is more complex than that seen in low disorder samples. f_{pk} increases with decreasing ν as ν goes below 0.8 and a maximum in f_{pk} vs ν occurs for ν just below $3/4$. The CF picture provides possible explanations of the features. The disorder extends the ν range of the existence of the resonance, so that there is reentrance at least of a highly damped resonance, around FQHE states.

We thank Kun Yang and J. K. Jain for helpful discussions and A. T. Hatke for his comments on the manuscript. The work at Princeton was funded through the NSF through MRSEC DMR-0819860 and the Keck Foundation and the Gordon and Betty Moore Foundation (grant GBMF4420). The microwave spectroscopy work at NHMFL was supported through DOE grant DE-FG02-05-ER46212 at NHMFL/FSU. NHMFL is supported by NSF Cooperative Agreement No. DMR-0084173, the State of Florida and the DOE.

¹ Y. E. Lozovik and V. I. Yudson, JETP Lett., **22**, 11 (1975).

² P. K. Lam and S. M. Girvin, Phys. Rev. B **30**, 473 (1984).

³ Kun Yang, F. D. M. Haldane, and E. H. Rezayi Phys. Rev. B **64**, 081301 (2001).

⁴ R. Narevich, Ganpathy Murthy, and H. A. Fertig, Phys. Rev. B **64**, 245326 (2001).

⁵ Chia-Chen Chang, Csaba Töke, Gun Sang Jeon, and Jainendra K. Jain Phys. Rev. B **73**, 155323 (2006); Chia-Chen Chang, Gun Sang Jeon, and Jainendra K. Jain Phys. Rev. Lett. **94**, 016809 (2005).

⁶ Alexander C. Archer and Jainendra K. Jain Phys. Rev. B **84**, 115139 (2011).

⁷ A. C. Archer, Kwon Park, Jainendra K. Jain, Phys. Rev. Lett., **111**, 146804 (2013).

- ⁸ H. W. Jiang, R. L. Willett, H. L. Stormer, D. C. Tsui, L. N. Pfeiffer, and K. W. West, Phys. Rev. Lett., **65**, 633 (1990).
- ⁹ V. J. Goldman, M Santos, M Shayegan, and J. E. Cunningham, Phys. Rev. Lett. **65**, 2189 (1990).
- ¹⁰ E. Y. Andrei, G. Deville, D. C. Glattli, F. I. B. Williams. E. Paris, and B. Etienne, Phys. Rev. Lett. **60**, 2765 (1988).
- ¹¹ H. Buhmann, W. Joss, K. v. Klitzing, I. V. Kukushkin, A. S. Plaut, G. Martinez, K. Ploog, and V. B. Timofeev, Phys. Rev. Lett. **66**, 926 (1991).
- ¹² I. V. Kukushkin, Vladimir I. Falko, R. J. Haug, K. von Klitzing, K. Eberl, and K. Ttemayer Phys. Rev. Lett. **72**, 3594(1994).
- ¹³ F. I. B. Williams, P. A. Wright, R. G. Clark, E. Y. Andrei, G. Deville, D. C. Glattli, O. Probst, B. Etienne, C. Dorin, C. T. Foxon, and J. J. Harris, Phys. Rev. Lett. **66**, 3285 (1991).
- ¹⁴ M. A. Paalanen, R. L. Willett, R. R. Ruel, P. B. Littlewood, K. W. West, L. N. Pfeiffer and D. J. Bishop, Phys. Rev. B **45**, 11342 (1992).
- ¹⁵ M. A. Paalanen, R. L. Willett, R. R. Ruel, P. B. Littlewood, K. W. West, L. N. Pfeiffer and D. J. Bishop, Phys. Rev. B **45**, 13784 (1992).
- ¹⁶ L. W. Engel, C.-C. Li, D. Shahar, D. C. Tsui and M. Shayegan, Solid State Commun., **104** 167-171 (1997).
- ¹⁷ C.-C. Li, J. Yoon, L. W. Engel D. Shahar, D. C. Tsui and M. Shayegan, Phys. Rev. B **61**, 10905 (2000).
- ¹⁸ P. D. Ye, L. W. Engel, D. C. Tsui, R. M. Lewis, L. N. Pfeiffer, and K. West, Phys. Rev. Lett. **89**, 176802 (2002).
- ¹⁹ G. Sambandamurthy, Zhihai Wang, R. M. Lewis, Yong P. Chen, L. W. Engel, D. C. Tsui, L. N. Pfeiffer and K. W. West, Solid State Commun. **140**, 100 (2006) contains a brief review.
- ²⁰ M. Shayegan, in Perspectives in Quantum Hall Effects, edited by S. Das Sarma and A. Pinczuk (Wiley-Interscience, New York, 1997), p. 343.
- ²¹ Yong Chen, R. M. Lewis , L. W. Engel , D. C. Tsui , P. D. Ye , L. N. Pfeiffer and K. W. West, Phys. Rev. Lett. **91**, 016801 (2003).
- ²² Han Zhu, G. Sambandamurthy, Yong P. Chen, P. Jiang, L. W. Engel, D. C. Tsui, L. N. Pfeiffer, and K. W. West, Phys. Rev. Lett. **104**, 226801 (2010).
- ²³ R. M. Lewis, Yong Chen, L. W. Engel, D. C. Tsui, P. D. Ye, L. N. Pfeiffer and K. W. West,

Physica E **22**, 104 (2004).

- ²⁴ L. Tiemann, T. D. Rhone, N. Shibata, and K. Muraki, Nat. Phys. **10**, 648 (2014).
- ²⁵ A. T. Hatke, Yang Liu, B. A. Magill, B. H. Moon, L. W. Engel, M. Shayegan, L. N. Pfeiffer, K. W. West and K. W. Baldwin, Nature Commun. **5**, 4154, (2014).
- ²⁶ Han Zhu, Yong P. Chen, P. Jiang, L. W. Engel, D. C. Tsui, L. N. Pfeiffer, and K. W. West, Phys. Rev. Lett. **105**, 126803 (2010).
- ²⁷ R. M. Lewis, P. D. Ye, L. W. Engel, D. C. Tsui, L. Pfeiffer, and K. W. West, Phys. Rev. Lett. **89**, 136804 (2002).
- ²⁸ Hidetoshi Fukuyama and Patrick A. Lee, Phys. Rev. B **18**, 6245 (1978).
- ²⁹ R. Chitra, T. Giamarchi, and P. Le Doussal, Phys. Rev. Lett. **80**, 3827 (1998); R. Chitra, T. Giamarchi, and P. Le Doussal, Phys. Rev. B **65**, 035312 (2001).
- ³⁰ H. A. Fertig, Phys. Rev. B **59**, 2120 (1999).
- ³¹ M. M. Fogler, and D. A. Huse, Phys. Rev. B **62**, 7553 (2000).
- ³² Wanli Li, D. R. Luhman, D. C. Tsui, L. N. Pfeiffer, and K. W. West, Phys. Rev. Lett. **105**, 076803 (2010).
- ³³ Wanli Li, G. A. Csáthy, D. C. Tsui, L. N. Pfeiffer, and K. W. West, Appl. Phys. Lett. **83**, 2832 (2003).
- ³⁴ Wanli Li, G. A. Csáthy, D. C. Tsui, L. N. Pfeiffer, and K. W. West, Phys. Rev. Lett. **94**, 206807 (2005).
- ³⁵ Wanli Li, C. L. Vicente, J. S. Xia, W. Pan, D. C. Tsui, L. N. Pfeiffer, and K. W. West, Phys. Rev. Lett. **102**, 216801 (2009).
- ³⁶ Wanli Li, J. S. Xia, C. Vicente, N. S. Sullivan, W. Pan, D. C. Tsui, L. N. Pfeiffer, and K. W. West, Phys. Rev. B **81**, 033305 (2010).
- ³⁷ B.-H. Moon, L. W. Engel, D. C. Tsui, L. N. Pfeiffer, and K. W. West, Phys. Rev. B **89**, 075310 (2014).
- ³⁸ D. Shahar, D. C. Tsui, M. Shayegan, R. N. Bhatt, and J. E. Cunningham Phys. Rev. Lett. **74**, 4511.
- ³⁹ Zhihai Wang, Yong P. Chen, Han Zhu, L. W. Engel, D. C. Tsui, E. Tutuc, and M. Shayegan, Phys. Rev. B **85**, 195408 (2012)
- ⁴⁰ N. W. Ashcroft and N. D. Mermin, *Solid State Physics* , (Saunders, Philadelphia, 1976).
- ⁴¹ S. E. Barrett, G. Dabbagh, L. N. Pfeiffer, K. W. West, and R. Tycko, Phys. Rev. Lett **74**, 5112

(1995).

- ⁴² S. L. Sondhi, A. Karlhede, S. A. Kivelson, and E. H. Rezayi, Phys. Rev. B **47**, 16419 (1993).
- ⁴³ A. Schmeller *et al.*, Phys. Rev. Lett. **75**, 4290 (1995).
- ⁴⁴ V. Bayot, E. Grivei, S. Melinte, M. B. Santos, and M. Shayegan, Phys. Rev. Lett. **76**, 4584 (1996); **79**, 1718 (1997); S. Melinte, E. Grivei, V. Bayot, and M. Shayegan, *ibid.* **82**, 2764 (1999).
- ⁴⁵ R. Côté, A. H. MacDonald, Luis Brey, H. A. Fertig, S. M. Girvin, and H. T. C. Stoof, Phys. Rev. Lett. **78**, 4825 (1997).
- ⁴⁶ R. Price, Xuejun Zhu, P. M. Platzman, and Steven G. Louie, Phys. Rev. B **48**, 11473 (1993).
- ⁴⁷ Yong P. Chen, G. Sambandamurthy, Zhihai Wang, R. M. Lewis, L. W. Engel, D. C. Tsui, P. D. Ye, L. N. Pfeiffer, K. W. West, Nature Physics **2**, 425-455 (2006).
- ⁴⁸ J. K. Jain, *Composite Fermions*. Cambridge University Press, Cambridge, 2007.
- ⁴⁹ B. I. Halperin, Patrick A. Lee, and Nicholas Read Phys. Rev. B **47**, 7312 (1993).
- ⁵⁰ R. Chitra and T. Giamarchi Eur. Phys. J. B **44**, 455467 (2005).
- ⁵¹ S. Ilani, J. Martin, E. Teitelbaum, J. H. Smet, and D. Mahalu, Nature **427**, 328 (2004).
- ⁵² Reza Jamei, Steven Kivelson, and Boris Spivak, Phys. Rev. Lett. **94**, 056805 (2005).
- ⁵³ Boris Spivak and Steven A. Kivelson Phys. Rev. B **70**, 155114 (2004).